New Catalysts of the Metal–Filamentary Carbon Type: From Fundamental Research to Technology

V. V. Molchanov, V. V. Chesnokov, R. A. Buyanov, N. A. Zaitsev, and V. I. Zaikovskii

Boreskov Institute of Catalysis, Siberian Division, Russian Academy of Sciences, Novosibirsk, 630090 Russia

Received October 28, 2004

Abstract—A principally new basic catalytic system is developed. The system is based on dispersed metal particles incorporated into carbon filaments by the catalytic decomposition of hydrocarbons on these particles. The basic system enables one to synthesize a series of catalysts for different processes. Mechanisms and methods for controlling the catalytic properties of this system are studied. The role of the crystal faces of the metal particles and of chemisorbed hydrogen species in selective hydrogenation is established. The chemical composition of the active component is optimized for the removal of acetylene from ethylene and of butadiene from butenes. A technology for catalyst precursor preparation is developed, which includes a mechanochemical activation stage and the shaping of the resulting powder. Optimum conditions are found for hydrocarbon decomposition in order to obtain metal–carbon catalysts for selective hydrogenation.

For a long time, the formation of filamentary carbon on iron-family metals was viewed as a harmful phenomenon accompanying petroleum refining and petrochemical processes. However, useful properties of filamentary carbon and several applications of this material have been discovered in the last 15 years. Materials based on filamentary carbon have found use as sorbents [1, 2], catalyst supports [3, 4], and structural materials [5]. The number of publications on the methods of preparation and properties of filamentary carbon has recently increased sharply.

The materials considered here contain metal particles catalyzing hydrocarbon decomposition into hydrogen and filamentary carbon. The authors of this publication were the first to study metal particles bound to carbon filaments under the assumption that they can be an active component, as in supported catalysts [6].

Filamentary carbon consists of solid or hollow filaments at the ends of which metal particles are fixed (Fig. 1). Therefore, these particles can possess special catalytic properties. No similar conceptions were earlier advanced, except for a publication in which the catalytic activity in the Fischer–Tropsch reaction was ascribed to iron dispersed in carbon forming in this process [7]. However, this conclusion seems doubtful on analysis of the experimental data presented in [7].

These new catalysts are prepared by catalytic hydrocarbon decomposition, an unconventional method. Varying the nature of the original catalyst allows one to synthesize metal–carbon systems with a metal content of 0.25 to 90 wt %. The size of metal particles varies between 7 and 50 nm, depending on synthesis conditions. As is shown below, the active component can contain V, Mn, Cu, Zn, Mo, Ru, Pd, In, Sn, Pt, and apparently other metals along with iron-family metals.

The nature of the hydrocarbon being decomposed affects the morphology of both the metal particles and the carbon filaments. The multiplicity of variable parameters allows catalytic systems to be designed for particular reactions.

FUNDAMENTAL RESEARCH

Since the active components are metals, it is natural to assume that the catalysts under consideration will be active in reactions typical for metallic catalysts. The early experiments confirmed these assumptions. We studied the catalytic properties of metal–filamentary carbon systems in reactions traditionally catalyzed by supported metals. These systems are active in steam and CO_2 methane conversion, the Fischer–Tropsch reaction, CO methanation, butane dehydrogenation, the reductive dechlorination of chlorobenzene, the oxidation of CO and hydrogen, and the hydrogenation of unsaturated hydrocarbons and fatty acids [7]. The most interesting results were obtained for steam methane conversion, CO oxidation, and unsaturated hydrocarbon hydrogenation. Let us consider these processes in greater detail.

Steam Methane Conversion

The procedure for the determination of catalytic activity in steam methane conversion is described elsewhere [8]. Activities were compared in terms of the reaction rate constant per unit weight of active metal.

The initial activity of the resulting materials exceeded the activity of the commercial catalyst GIAP-16 (Table 1). However, their activity decreased with time, most probably due to coking. Under these condi-
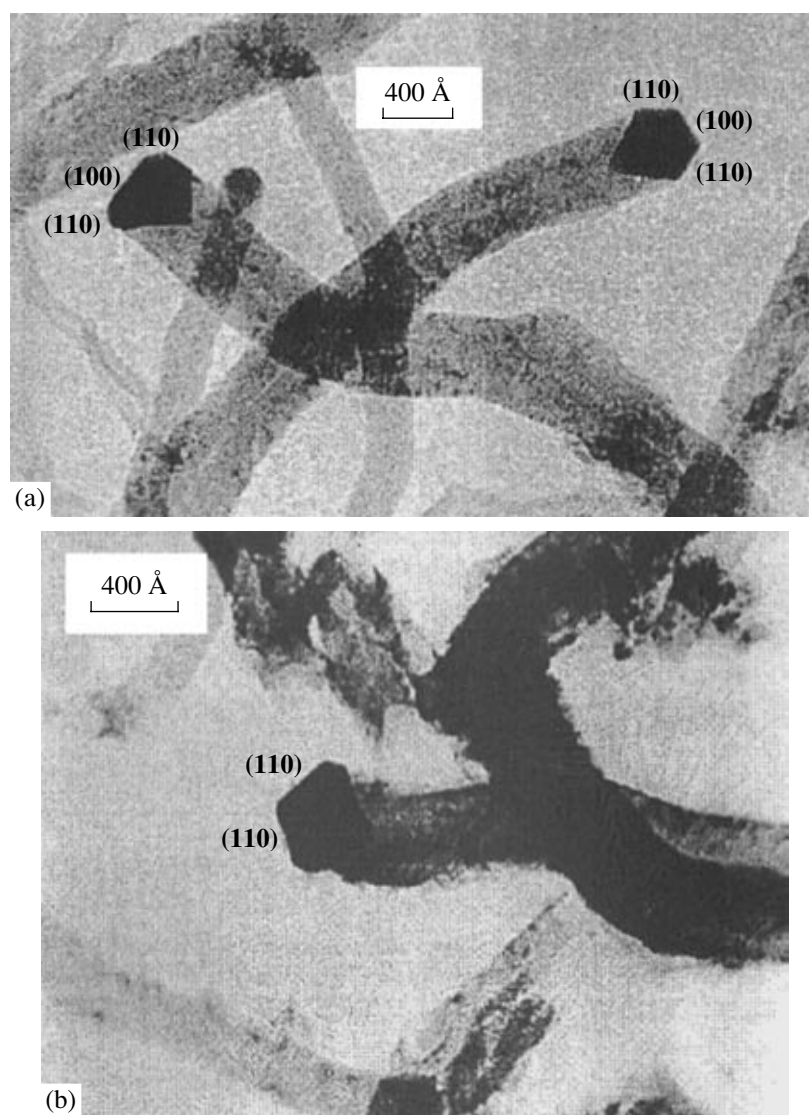
Fig. 1. Electron micrographs of the Ni–filamentary carbon specimens. C/Ni = (a) 1.5 and (b) 10.

tions, the operation of the commercial catalyst is more stable. Nevertheless, we consider it pertinent to continue research in this field.

CO Oxidation

Carbon monoxide was oxidized in a loop flow reactor at 623 K. The catalyst weight was 2 g, and the flow rates of CO and air were 2.5 and 6 l/h, respectively. Catalytic activities were compared in terms of reaction rate per unit surface area. In the case of the metal–carbon catalysts, the rate was calculated for the metal surface area determined from oxygen chemisorption data. The determination of specific surface area is described in [9]. The catalytic activity data are listed in Table 2. It was shown by special experiments that carbon does not oxidize under the reaction conditions.

Hydrogenation of Unsaturated Compounds

The hydrogenation of unsaturated fatty acids and unsaturated hydrocarbons was studied. Unsaturated

Table 1. Rate constants of steam methane conversion on various catalysts as a function of testing time

Catalyst	Rate constant $((cm^3 CH_4) g^{-1} atm^{-1} s^{-1})$ at various test durations, h		
	0	5	10
Ni/C (60 wt % Ni)	26	20	13
Ni/C (50 wt % Ni)	32	25	11
GIAP-16 (Ni/Al$_2$O$_3$)	20	18	16

Table 2. Specific rate of CO oxidation on the metal–carbon catalysts and on Fe_2O_3

Catalyst	Reaction rate, 10^8 (mol CO) m^{-2} s^{-1}
15% Fe/C	302
23% Co/C	271
Fe_2O_3	5.5

Note: $T = 623$ K; $CO/O_2 = 2 : 1$.

Table 3. Specific rate and the selectivity of butadiene hydrogenation on the metal–carbon catalysts

Catalyst	Reaction rate $\times 10^6$, (mol C_4H_6) g^{-1} s^{-1}	C_4H_8 selectivity, mol %
15% Fe	85.6	99.4
23% Co	71.2	91.0
4.2% Ni	74.5	99.5*
55% Ni	403	99.1*
2.8% $Ni_{0.9}Cu_{0.1}$	200	99.1
0.25% $Ni_{0.9}Cu_{0.1}$	2055	100
Pd/Al_2O_3 (MA-15)	1015	72.0

Note: $T = 473$ K; $H_2/C_4H_6 = 5 : 1$.
   * C_4H_{10} selectivity.

Table 4. Specific rate and the selectivity of acetylene hydrogenation on the metal–carbon catalysts

Catalyst	Reaction rate $\times 10^6$, (mol C_2H_2) g^{-1} s^{-1}	C_2H_4 selectivity, mol %
55% Ni	6.3	74.0
0.25% $Ni_{0.9}Cu_{0.1}$	303	99.8
18% $Fe_{0.64}Ru_{0.36}$	16.9	99.5
Pd/Al_2O_3 (MA-15)	1040	43.0

Note: $T = 423$ K, $H_2/C_2H_2 = 5 : 1$.

hydrocarbons were hydrogenated in a loop flow reactor at 293–473 K. The catalyst weight was 0.2 g, and the flow rates of hydrogen and unsaturated hydrocarbons were 7 and 1.4 l/h, respectively. The catalytic properties of samples were estimated in terms of reaction rate per unit weight of active metal and in terms of olefin selectivity.

Benzene was hydrogenated in a flow reactor at 573 K and a hydrogen pressure of 1.96 MPa.

Unsaturated fatty acids were hydrogenated in a stirred autoclave at 420 K and an initial hydrogen pressure of 1.47 MPa. Catalytic activity was estimated from the change in the hydrogen pressure in the autoclave.

The activity of the metal–carbon catalysts in the hydrogenation of fatty acids was lower than the activity of the commercial catalyst GM-3. Perhaps, this is due to the fact that the metal surface is not reduced under the reaction conditions. More interesting results were obtained for the hydrogenation of unsaturated hydrocarbons.

The following interesting feature of the metal–carbon catalysts cannot be explained by available data: the benzene ring is hydrogenated on none of these catalysts, although supported nickel catalysts, including those on the carbon supports, exhibit a rather high activity in this reaction. This property can be used in the selective hydrogenation of substituents in aromatic compounds. We have demonstrated that the hydrogenation of *p*-benzoquinone into hydroquinone, nitrobenzene into aniline, and benzamide into benzylamine occur on the metal–carbon catalysts with a selectivity close to 100% [10].

Among the hydrogenation reactions, the selective hydrogenation of acetylenes and dienes into olefins is of special interest. These reactions have practical significance: they are used for the purification of raw materials for the production of rubbers and plastics. Presently, supported palladium or platinum catalysts are used for this purpose. To achieve an appropriate selectivity, they are treated with sulfur compounds, which are added to the raw materials as well. However, the low selectivity does not prevent high losses of the desired products. Therefore, it is evident that a search for new, more efficient catalysts is necessary. For this reason, having discovered new catalytic systems, we have attempted to apply them to the selective hydrogenation of dienes and acetylenes.

The specific catalytic activity of some metal–carbon catalysts in butadiene hydrogenation exceeds the activity of supported palladium (Table 3).

In acetylene hydrogenation, none of the metal–carbon catalysts exceeds the supported palladium in specific activity (Table 4).

The specific features of the metal–carbon catalysts are especially interesting in the selective hydrogenation of dienes and acetylenes into olefins. The properties of these catalysts depend on the amount of filamentary carbon formed on the metal. For low C : M ratios (M is a metal), complete hydrogenation occurs on these catalysts and some of them provide 100% conversion at room temperature. Unlike supported platinum and palladium catalysts with the same properties, the metal–carbon systems cause no hydrogenolysis. The olefin selectivity of acetylene and butadiene hydrogenation increases with an increase in C : M. We studied this effect in greater detail for butadiene hydrogenation on the Ni/C catalysts (Fig. 2). Figure 2 shows that the selectivity has a plateau at a certain C : Ni ratio. Similar plots were obtained for Ni–Cu/C and Ni–Pd/C catalysts. However, these catalysts have some specific features. The nickel–copper catalysts exhibit a high selec-

tivity even at small C : M ratios. At small C : M ratios, the nickel–palladium catalysts are intermediate between the nickel and nickel–copper catalysts in terms of selectivity. The selectivities of the three catalytic systems are nearly equal at large C : M ratios.

At large C : M values, the nickel catalysts with other additions also possess a high selectivity. The catalytic properties of the metal–carbon catalysts containing various transition metals are presented in Table 5.

The present views of the nature of the selectivity of the catalysts do not explain the plot shown in Fig. 2 or other catalytic properties of these systems described in [6, 11]. The sources of the selectivity of the metal–filamentary carbon catalysts were established by analysis of the changes in the metal particles caused by filamentary carbon formation [11]. The main factors in the catalytic activity and selectivity are the changes in the nature of the exterior metal crystal faces that are accessible to the reaction medium and the defect structure of the metal particles. The morphology of the particles changes due to the formation of filamentary carbon (the mechanism of this process is described in detail in [12]).

At the earliest stage of the carburization of samples, nickel particles, which have the shape of isometric crystals, are transformed into particles with a planar head part, as is shown in Fig. 1a. These particles are gradually transformed into particles with a sharpened head part with increasing C : Ni ratio (Fig. 1b). The shape of individual particles changes nonuniformly, and a small number of particles with the shape as in Fig. 1b appears already at small C : Ni values. For

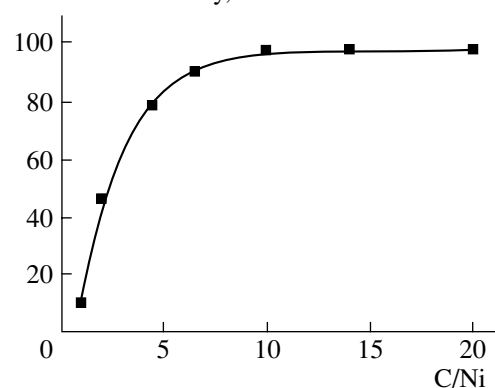*n*-Butene selectivity, mol %

Fig. 2. Butene selectivity versus C/Ni weight ratio.

example, about 90% particles of type 1a and 10% particles of type 1b are observed at C : Ni = 1.5. In the sample with C : Ni = 10, type 1b dominate, while type 1a particles are almost entirely absent.

The use of electron microdiffraction and measurement of angles between faces in the particles allowed us to identify these faces. Based on the data obtained, we can conclude that the ⟨100⟩ and ⟨110⟩ faces are accessible to the reaction mixture at small C : Ni values. At the same time, only the 110 face is accessible at large C : Ni ratios, because the 100 face disappears and the ⟨111⟩ face is blocked with carbon, as in the first case. This orientation of the metal particles is caused by the mechanism of filamentary carbon formation. According to this mechanism, hydrocarbons decompose into

Table 5. Catalytic properties of the metal–carbon catalysts in butadiene hydrogenation to butenes

Catalyst	C : M weight ratio	C_4H_6 conversion, mol %	C_4H_8 selectivity, mol %
$Ni_{0.9}Cu_{0.1}$	40	82	98.7
$Ni_{0.9}Cu_{0.1}$	400	70	100
Fe	5.5	77	99.4
Ni	23	17	99.1
$Ni_{0.93}Pd_{0.07}$	15	73	99.6
$Ni_{0.996}Pt_{0.004}$	32	42	98.9
$Ni_{0.9}Mo_{0.1}$	7	46.8	86.2
$Ni_{0.98}In_{0.02}$	5	71	99.0
$Ni_{0.98}Zn_{0.02}$	5	50	93
$Ni_{0.98}Sn_{0.02}$	5	77	96.6
$Ni_{0.98}Mn_{0.02}$	61	60	99.4
$Ni_{0.98}V_{0.02}$	61	68	98.8
$Ni_{0.85}Cu_{0.13}Fe_{0.02}$	183	34	95
MA-15 (Pd/Al_2O_3)*		36	72
Pd/C (Sibunit)*		92	74

Note: $T = 473$ K; $H_2/C_4H_6 = 5 : 1$.

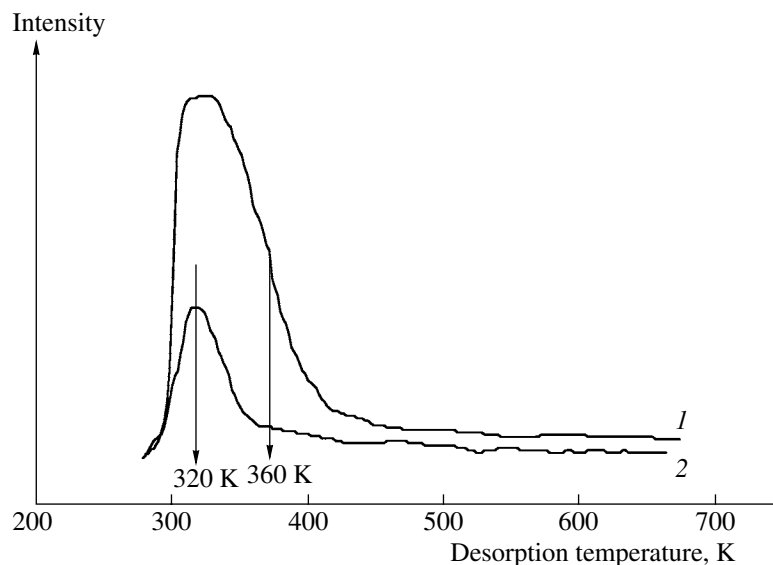 * The reaction temperature was 373 K, because at higher temperatures the selectivity decreased sharply.

Fig. 3. Hydrogen TPD spectra for the nickel–carbon catalysts with C/Ni ratios of (*1*) 1.5 and (*2*) 10.

carbon and hydrogen on the ⟨100⟩ face and then the carbon diffuses through the bulk of the metal particle and crystallizes as graphite on the ⟨111⟩ face. This is the reason why the ⟨111⟩ face is inaccessible to the reaction medium, as is well seen in electron micrographs (Figs. 1a, 1b). This change in the nature of the crystal faces accessible to the reaction medium should change the character of the chemisorption of hydrogen and hydrocarbons.

The exterior cutting of the metal particles is affected by the nature of the hydrocarbon used in catalyst preparation. This effect is described in detail in [13], and here we only mention that the well-faceted particles described above are formed in the case of hydrocarbons that decompose with heat absorption (methane, ethane, propane, and hexane). If the hydrocarbon decomposes with heat release, unfaceted, droplike metal particles result. The exterior surface of these particles is formed by steps of ⟨111⟩ faces, and such catalysts exhibit a low selectivity in hydrogenation even at large C : M ratios.

According to electron microdiffraction and electron microscopy data, for C : M ratios above 20, the particles are defective. For example, electron micrographs indicate ⟨111⟩ twinning boundaries and electron diffraction patterns show reflections characteristic of twins. For C : M ≈ 30, the roughness of the exterior faces of the metal crystallites increases due to the increase in their defectivity. The catalysts containing defect crystallites are highly selective and more active. For the nickel–copper catalyst, as C : Ni–Cu increases from 10 to 35, the hydrogenation rate per unit weight of the alloy increases by a factor of 2.5 (from 78 to 200×10^{-6} (mol C_4H_6) g^{-1} s^{-1}). As this ration is further increased to 400, the hydrgenation rate increases tenfold (to 2055×10^{-6} (mol C_4H_6) g^{-1} s^{-1}).

The state of hydrogen chemisorbed on the catalyst surface (hydrogen speciation) exerts a substantial effect on the catalytic reactions involving this hydrogen. We assumed (see above) that changes in the exterior faceting of the metal particles must affect hydrogen chemisorption. This assumption was confirmed by the temperature-programmed desorption of hydrogen. For C : Ni = 1.5, two desorption peaks are observed (Fig. 3): the peak at 360 K can be attributed to hydride hydrogen [14, 15], and the peak at 320 K is due to atomic hydrogen. For C : Ni = 10, no hydride hydrogen peak is observed and only a peak at 320 K is seen. Based on these data, we can assume that complete hydrogenation is due to the high reactivity of the hydride hydrogen involved in the reaction and the disappearance of this form with an increase in C : Ni enhances the selectivity of butadiene hydrogenation into butenes. Therefore, it is likely that the selectivity of the catalysts with a large C : M ratio also depends on the proportions of different hydrogen forms.

Interesting results confirming the above assumption as to the role of the hydride hydrogen were obtained by studying the influence of the reaction temperature and the thermal hydrogen pretreatment of the catalysts on the selectivity of the process. For C : Ni = 1.5, an increase in the temperature of butadiene hydrogenation from 408 to 493 K raises the butene selectivity from 54 to 98%. For the same sample, an interruption of the butadiene supply, followed by treating the catalyst with pure hydrogen at 493 K, decreases the selectivity to 77%. The hydrogen pretreatment temperature has a similar effect. For instance, the selectivity of the catalyst calcined in hydrogen at 473 K is 67%, while the selectivity of the catalyst calcined at 673 K is 91%.

Another argument in favor of the substantial effect of hydride hydrogen on the catalyst selectivity is provided by the properties of the samples obtained by butadiene decomposition on the nickel–copper alloy. For

the same ratio of C : Ni = 10, the butene selectivity of a specimen obtained in this way is much lower than that of the specimen prepared by methane decomposition (57 and 97%, respectively). The study of the former specimen by temperature-programmed hydrogen desorption showed that it contains hydride hydrogen. This fact explains the low selectivity of the specimen obtained by butadiene decomposition.

The possibility of hydride hydrogen formation depends on the electronic state of nickel. The samples having many defects in their metal particles have an electron density deficit on their surface. This impedes electron transfer from the metal to hydrogen and prevents the formation of hydride hydrogen. This is the reason why the butadiene selectivity of the catalysts obtained by butadiene decomposition is 57% at C : Ni = 10, 96% at C : Ni = 80, and 100% at C : Ni = 400.

PASSING TO THE TECHNOLOGY OF PREPARATION OF CATALYSTS FOR THE REMOVAL OF ACETYLENES AND DIENES FROM MONOMERS

The high selectivities shown by the metal–filamentary carbon catalysts encouraged us to use them in the removal of acetylens and dienes from monomers. This is a serious problem of industrial polymer production. Very small amounts of acetylenes and dienes in monomers worsens the quality of the resulting polymers and deactivates the polymerization catalysts.

Of the variety of known purification methods, extractive distillation and selective hydrogenation of the impurities are the most popular. The advantages of selective hydrogenation are its low energy intensity and the absence of wastewater or bulky equipment. The most efficient catalysts for selective hydrogenation are supported palladium catalysts. They have three main disadvantages: high cost, low selectivity resulting in a loss of desired products, and side resinification processes (the formation of so-called green oil). The latter decreases the activity and requires regular regeneration. Palladium-free catalysts are not widespread because of their lower activity along with the above disadvantages. Therefore, the creation of commercial catalysts that contain no noble metals but are efficient in the removal of harmful impurities and possess none of the above disadvantages would be a marked progress. This could be achieved by the discovery and study of new metal–filamentary carbon catalysts.

Experiments on the purification of industrially used and model mixtures showed that the new catalysts are highly efficient, as is demonstrated by the data presented in Tables 6–8.

These data convinced us of the need for designing a process for the manufacture of metal–filamentary carbon catalysts.

Table 6. Acetylene removal from ethylene*

Sample	T, K	C_2H_2 content after purification, mol %
2.5% Ni	413	0.0003
2.6% $Ni_{0.8}Cu_{0.2}$	373	0.0020
	393	0.0001
5.2% $Ni_{0.86}V_{0.14}$	363	0.0001

* The initial mixture contained 0.025 mol % C_2H_2. C_2H_6 was observed after purification in none of the cases.

Table 7. Removal of butadiene from butenes*

Sample	T, K	Content after purification, mol %	
		C_4H_6	C_4H_{10}
0.25% $Ni_{0.9}Cu_{0.1}$	423	<0.003	11.2
6.3% Fe	473	<0.003	11.2

* The starting mixture contained 1.05 mol % C_4H_6 and 11.3 mol % C_4H_{10}.

Table 8. Removal of acetylenes from a butene–butadiene mixture*

Sample	T, K	C_4H_6 content after purification**, mol %
		C_4H_6
0.25% $Ni_{0.9}Cu_{0.1}$	373	42.3
2.6% $Ni_{0.8}Cu_{0.2}$	348	43.8
5.5% $Ni_{0.9}Cu_{0.1}$	303	44.5
6% $Ni_{0.93}Pd_{0.07}$	353	43.2
6.3% Fe	433	43.6

* The initial mixture contained 0.23 mol % acetylenes ($\Sigma C \equiv C$) and 43.6 mol % C_4H_6.
** After purification, $\Sigma C \equiv C$ was <0.003 mol %.

In our opinion, the following three problems need to be solved for this purpose:

(1) Optimization of the active component for the hydrogenation of particular impurities and development of a technology for producing precursor catalysts (i.e., catalysts for hydrocarbon decomposition).

(2) Design of an industrial process for catalytic hydrocarbon decomposition yielding hydrogen and a metal–carbon material.

Table 9. Results of testing the metal–carbon catalysts in the removal of acetylene from ethylene

Active component	C : M weight ratio	Minimum temperature for purification to a C_2H_2 content of 10 ppm, K	Onset temperature of C_2H_6 formation, K
$Ni_xE_y^*$	–	353	385
$Ni_{0.857}Cu_{0.143}$	8.5	373	385
$Ni_{0.964}Cu_{0.036}$	12.0	368	378
$Ni_{0.964}Mn_{0.036}$	13.0	363	373
$Ni_{0.952}Mn_{0.048}$	12.5	363	383
$Ni_{0.952}V_{0.048}$	11.0	348	348
$Ni_{0.857}V_{0.143}$	11.8	363	373

* E stands for modifiers ensuring the highest catalyst efficiency. Information concerning these additives is confidential.

Table 10. Results of testing the metal–carbon catalysts in the removal of butadiene from *n*-butene

Active component	C : M weight ratio	Minimum temperature for purification to a C_4H_6 content of 10 ppm, K	Onset temperature of C_4H_{10} formation, K
$Ni_{0.952}Mn_{0.048}$	12.5	365	373
$Ni_{0.952}V_{0.048}$	11	383	383
$Ni_xE_y'^*$	–	348	373
$Ni_{0.952}Cu_{0.048}$	8.5	368	368

* E' stands for modifiers ensuring the highest catalyst efficiency. Information concerning these additives is confidential.

(3) Development of a technology for producing shaped metal–carbon catalysts.

Optimization of the Composition of the Active Component

The optimization of the composition of the active component has been based on the above fundamental results. Several elements alloyable with nickel and manifesting the highest selectivity in the processes of interest were considered, and the composition of the active component was optimized for the efficient removal of a particular impurity. Beginning our studies, we proceeded from the assumption that the composition of the active component optimal for acetylene removal from ethylene must differ from the optimal composition for butadiene removal from butene because acetylene and butadiene are very different in terms of structure and properties. These studies confirmed this assumption. To optimize the active component, we varied the nature and amount of the element to be alloyed with nickel.

Parameters important to both processes are purification depth and the difference between the minimum temperature at which the desired purification efficiency is achieved and the temperature at which the products of complete hydrogenation (ethane and butane) appear. Therefore, in the case of catalyst deactivation, it is possible to increase the reaction temperature without los-

ing desired products. For commercial palladium catalysts, these temperatures differ almost not at all and, hence, substantial losses take place. The results of our tests are given in Tables 9 and 10.

The data in Tables 9 and 10 show that, for both processes, we succeeded in selecting compositions that ensured efficient purification at a considerable difference between the minimum temperature at which the desired purification efficiency is achieved and the onset temperature of complete hydrogenation.

Developing a Technology for Precursor Catalyst Production

The metal–carbon catalysts are produced by the decomposition of hydrocarbons on precursor catalysts containing iron-family metals (primarily nickel) or their alloys with other metals. A necessary condition for the efficient formation of filamentary carbon is that the metal or alloy particles are not larger than 50 nm. We attempted to prepare such particles using mechanochemical activation in planetary mills. It was necessary to comminute nickel oxide or its mixture with other oxides to the desired particle size and to prevent the agglomeration of metal or alloy particles both during reduction and during the subsequent reaction. To solve these problems, we introduced compounds with a layered structure (magnesium or aluminum hydroxide or graphite) into the activated mixtures. These proce-

dures made it possible to obtain highly efficient catalysts for methane decomposition. Note that the precursor preparation procedure that included a mechanochemical activation stage afforded the most efficient purification catalysts. The activation time, the rotational speed of the drum, and the ratio between the batch and the activated mixture were optimized.

Using the optimized data, we developed a technology for precursor catalyst production, which includes the following steps:

mechanochemical activation of a mixture of oxides and hydroxides,

extrusion of activated powders with a plasticizer and a binder,

drying, and

calcination.

Thus, we have presented the initial data necessary for the design of a process for precursor catalyst production.

Developing a Process for the Catalytic Decomposition of Hydrocarbons Yielding Hydrogen and a Metal–Carbon Material

Solving this problem, one should take into account that the volume of the catalyst increases considerably (by a factor of up to 30) due to carbon formation during hydrocarbon decomposition. Therefore, the process cannot be carried out in a fixed catalyst bed because of the risk of reactor breaking. The reaction should be carried out either in a reactor with a large free volume or in a moving-bed reactor. There are four variants of reactor design to be tested: (1) fixed thin bed of precursor catalyst on trays, (2) catalyst bed fluidized with natural gas, (3) vibrated fluidized bed, and (4) rotating reactor. The reaction in a fluidized-bed reactor requires precursor catalyst granules to have a high abrasion resistance. Of the catalysts used, only supported systems satisfy this requirement. However, they do not have the necessary catalytic properties and, therefore, we must reject this method. The hydrogenation catalysts obtained in a vibrated fluidized bed, though rather selective, show a low activity for reasons that are not understood. The catalysts with the same catalytic properties were obtained in fixed-bed and rotating reactors. However, the rotating reactor, unlike the flow reactor with plates, has no concentration gradients and thus affords providing a more uniform distribution of the resulting carbon and active components over the granules. For this reason, the metal–carbon catalysts were produced in a 250-cm^3 rotating reactor.

Another task was to select cheap hydrocarbon raw materials for the preparation of the metal–carbon catalysts. It was preliminarily established that selective catalysts result only from C_1–C_3 hydrocarbons. Therefore, the cheapest raw materials, which are hydrocarbon mixtures to be flared, turned out to be inappropriate and natural gas was chosen as a crude. Special experiments

showed that the regularities of metal–carbon material formation by methane decomposition are rather well reproduced when natural gas is used in place of methane.

To optimize the conditions for the preparation of selective hydrogenation catalysts based on filamentary carbon, we varied the following parameters: temperature, carbonation time, and natural gas flow rate. The optimum temperature range for natural gas decomposition is 550–650°C for the following reasons. On the one hand, below 550°C, the reaction rate decreases sharply and the degree of methane decomposition and the yield of filamentary carbon decrease because of thermodynamic limitations. On the other hand, above 650°C, the process is energetically unfavorable and, more importantly, the nickel crystals lose their faceting, assuming the shape of drops. This has an adverse effect on the selectivity of hydrogenation of dienes and acetylene. The amount of catalyst to be charged into the reactor was optimized so as to obviate reactor clogging with the carbon filaments. The optimum initial catalyst charge was 1–2 g. The optimum flow rate of natural gas was 50 l/(g Cat). Decreasing this rate considerably lengthened the process time, while increasing this rate resulted in a decrease in methane conversion and, accordingly, in the steady-state hydrogen concentration in the reactor. As a result, the growth rate of filamentary carbon increased, which exerted an adverse effect on the faceting of the nickel particles. Under the optimized conditions, the reaction time was 4 h. The amount of deposited filamentary carbon reached 1000% of the weight of the starting catalyst, which is the optimum parameter for achieving the best selectivity at a sufficient activity. Based on our studies, we scaled up the laboratory-scale catalyst plant [6, 11] by a factor of ~300. Further scaling is now in progress.

CONCLUSIONS

Fundamental research has made it possible to develop a principally new catalytic system based on dispersed metal particles incorporated into carbon filaments by the catalytic decomposition of hydrocarbons on these particles. Using the base catalyst system, one can prepare a series of catalysts for various processes. The mechanisms and methods of control of the catalytic properties of the basic system were studied. The efficiency of the base system is particularly pronounced in the selective hydrogenation of acetylene and butadiene.

The selectivity of the metal–filamentary carbon catalysts in the hydrogenation of dienes and acetylenes is determined by the metal crystal faces accessible to the reaction medium. In the case of nickel particles, the ⟨110⟩ face is responsible for selective hydrogenation and the ⟨111⟩ and ⟨100⟩ faces are responsible for complete hydrogenation. To attain a high selectivity, we developed a method for the selective screening of the ⟨111⟩ and ⟨100⟩ faces with carbon. The crystallographic characteristics and faceting of the active metal particles can be controlled by varying the degree of carbonation

and the nature of the coking agent during the synthesis of the metal–carbon system.

The role of hydride and atomic hydrogen species in the hydrogenation processes on the nickel–carbon catalysts was established. Hydride hydrogen, which appears preferentially on the ⟨111⟩ and ⟨100⟩ faces, ensures the complete hydrogenation of acetylenes and dienes into the corresponding alkanes, and atomic hydrogen on the ⟨110⟩ face is involved in selective hydrogenation.

Applied study of the catalytic system resulted in the establishment of the optimum chemical composition of the active component in catalysts for the removal of acetylenes from ethylene and butadiene from butenes.

A technology was developed for precursor catalyst preparation. It includes mechanochemical activation and shaping of the resulting powder. Initial data necessary to design a process for precursor catalyst production were obtained.

A rotating reactor for the catalytic decomposition of hydrocarbons was developed. The optimum conditions for the preparation of the metal–carbon catalysts for selective hydrogenation were found. The results obtained on the laboratory scale are reproduced upon ~300-fold scaling of the process for preparing the metal–carbon hydrogenation catalysts.

ACKNOWLEDGMENTS

REFERENCES

1. USSR Inventor's Certificate no. 1327957, *Byull. Izobret.*, 1987, no. 3.
2. Bagrii, E.I., Tret'yakov, V.F., Trusova, E.A., *et al.*, *Neftekhimiya*, 1991, vol. 31, no. 2, p. 236.
3. Simagina, V.I., Stoyanova, I.V., Yakovlev, V.T., *et al.*, *Proc. 4th Eur. East–West Conf. & Exhibition on Material & Process*, St. Petersburg, 1993, p. 20.
4. Baker, R.T.K. and Harris, P.S., *Chemistry and Physics of Carbon*, New York: Marcel Dekker, 1978, vol. 11, p. 83.
5. Downs, W.B. and Baker, R.T.K., *Carbon*, 1991, vol. 29, no. 8, p. 1173.
6. Molchanov, V.V., Chesnokov, V.V., Buyanov, R.A., and Zaitseva, N.A., *Kinet. Katal.*, 1998, vol. 39, no. 3, p. 407.
7. Shultz, J.F., Karn, F.S., Anderson, R.B., and Hofer, L.J.E., *Fuel*, 1961, vol. 40, no. 3, p. 181.
8. Bobrov, N.N., Bobrova, I.I., and Sobyanin, V.A., *Kinet. Katal.*, 1993, vol. 34, no. 4, p. 686.
9. Buyanova, N.E., Karnaukhov, A.P., Kefeli, L.M., *et al.*, *Kinet. Katal.*, 1967, vol. 8, no. 4, p. 868.
10. RF Patent 2096083, 1997.
11. Molchanov, V.V., Chesnokov, V.V., Buyanov, R.A., *et al.*, *Kinet. Katal.*, 1998, vol. 39, no. 3, p. 416.
12. Chesnokov, V.V., Zaikovskii, V.I., Buyanov, R.A., *et al.*, *Kinet. Katal.*, 1994, vol. 35, no. 1, p. 146.
13. Zaitseva, N.A., Molchanov, V.V., Chesnokov, V.V., *et al.*, *Kinet. Katal.*, 2003, vol. 44, no. 1, p. 140.
14. Savchenko, V.I. and Boreskov, G.K., *Kinet. Katal.*, 1968, vol. 9, no. 1, p. 142.
15. Christmann, R., Shober, O., Ertl, G., and Neumann, M., *J. Chem. Phys.*, 1974, vol. 60, no. 11, p. 4528.